Synthesis and Electrochemical Characterization of AgNP Ink Suitable for Inkjet Printing

S. Milardović[1,*], I. Ivanišević[1], A. Rogina[2] and P. Kassal[1]

[1] Dept. of General and Inorganic Chemistry, Faculty of Chemical Engineering and Technology, University of Zagreb, Marulićev trg 19, HR-10000 Zagreb, Croatia
[2] Dept. of Inorganic Chemical Technology and Nonmetals, Faculty of Chemical Engineering and Technology, University of Zagreb, Marulićev trg 20, HR-10000 Zagreb, Croatia
E-mail: stjepan.milardovic@fkit.hr

To meet the growing demand for inkjet printable nanoparticle-based conductive inks, novel synthetic approaches are needed. In this study, spherical silver nanoparticles (AgNPs) with a mean diameter of approximately 2.5 nm were synthesized by the reduction of silver nitrate using an aqueous hydrazine solution in the presence of poly(acrylic acid) as a capping agent. The main goal of this work was the implementation of cyclic voltammetry as an electrochemical method for studying both the absorption of poly(acrylic acid) on the grain surface and nanoparticle interactions. The same technique was used to determine equimolar additions of hydrazine to obtain a high yield of reduced silver. All solutions used in the experiments were prepared at a high molar concentration. Silver nanoparticle-based ink was prepared by dispersing dried nanoparticles into a mixture of water and ethylene glycol and was stable for over seven months. For a comprehensive study of the prepared nanoink, UV-visible and electronic microscopy measurements were carried out. An inkjet technology was applied to deposit conductive ink to form linear silver tracks on a flexible substrate. These tracks exhibited a resistivity of 8.0×10^{-8} Ωm.

1. INTRODUCTION

Nanoparticles have been used in many different scientific fields such as materials science, electronics, medicine and biotechnology [1-7].

In the last decade, the silver nanoparticle literature has expanded exponentially, particularly work dealing with the development of stabilized particles suitable for inkjet printing technology. The

reason is the broad applicability of such nanoparticle-based inks. Inkjet printing of AgNPs has been applied for the printing of radio-frequency identification (RFID) devices [8], sensors [9,10], flexible displays [11], flexible electronics [12], printed batteries [13], microelectromechanical systems (MEMS) [14] micro-optics [15] and printed memories [16].

This technology can be adopted for printing on flexible substrates, such as plastics and paper, or for printing on solid substrates, such as glass, ceramics and metal.

Metal nanoparticles can be prepared and stabilized by chemical [17], physical [18] and biological methods [19-21]. Although there are several different chemical methods for silver nanoparticle preparation, the predominantly used method is wet synthesis. This synthesis is based primarily on silver nitrate reduction [22,23] by a certain reduction agent [24-26] in the presence of a capping agent [27] for grain size stabilization and homogenization.

The most frequently used reduction agents are trisodium citrate ($Na_3C_6H_5O_7$) [28,29], ascorbic acid ($C_6H_8O_6$) [30], sodium borohydride ($NaBH_4$) [31], hydrazine (N_2H_4) [32], hydroxylamine (NH_2OH) [33], ethylene glycol [34], aldehyde [35] polyols [36] and glucose [37]. The reducing agents act as electron donors and reduce the silver ions to their metal forms. The most commonly used capping agents include citrate, thiols [38,39], polymers such as poly(acrylic acid) [40-42], polyvinylpyrrolidone (PVP) [43], and poly(vinyl sulfonate) (PVS), compounds containing amino groups (NH_2^-) [44] and some surfactants [45,46]. Some of these agents function by covering the nanograins, forming a surface protection layer to prevent agglomeration, while others cause electrostatic repulsion between the nanograins. A major drawback of most of the mentioned wet syntheses is the use of highly diluted solutions, which makes these syntheses impractical for large scale production.

In the presented study, we attempt to produce Ag nanoink for inkjet printing [47-50] using concentrated solutions. The chemical reduction process that we used is based on silver nitrate reduction by hydrazine. The impact of poly(acrylic acid) used as a capping agent was studied by cyclic voltammetry. To the authors' knowledge, this is the first time this method was used to study the presence of a capping agent on silver nanoparticles. The same method was applied to determine the stoichiometric addition of hydrazine needed for total silver reduction. The properties of silver nanoparticles were tested by dynamic light scattering (DLS), transmission electron microscope (TEM) and UV-Vis measurements to determine and regulate the size distribution, zeta potentials and stability of the ink formulation during the testing period of seven months. The formulated nano-silver ink was printed on flexible plastic and paper substrates by means of an inkjet printer. In addition, to test the practical applicability of the developed ink formulation, the conductivity of the printed line shapes was determined.

2. EXPERIMENTAL SECTION

2.1. Materials

Silver nitrate ($AgNO_3$) was obtained from VWR Chemicals, Belgium and glacial acetic acid was obtained from BDH Prolabc, UK. Poly(acrylic acid) (PAA, $M_w = 1800$), hydrazine hydrate (50-60 wt%), ethylene glycol (EG; anhydrous, 99.8%), and 2-amino-2-methyl-1-propanol (2-AMP) were

purchased from Sigma-Aldrich (USA). Britton-Robinson (BR) buffer solutions were prepared from acetic acid (0.04 M), boric acid (0.04 M) and phosphoric acid (0.04 M), and the pH adjusted with NaOH. All chemicals used for BR buffer preparation were purchased from Kemika (Croatia). All chemicals were used as received without further purification. Deionized water was purified using a Millipore-MilliQ system.

The paper substrate for printing (glossy paper, photo quality, A4 formats) was obtained from Orink (China), while the plastic substrate (Novele^{TM}) was obtained from Novacentrix (USA). Both substrates were precoated by a top layer to enable low temperature sintering.

2.2. Instrumentation

All electrochemical experiments were performed using an EG&G PAR (USA) Model 264A Polarographic Analyzer and EDAQ (Australia) e-corder interfaced to a personal computer for data manipulation and data acquisition. A three-electrode electrochemical cell was used with a glassy carbon (GC, d = 3 mm) disc electrode as a working electrode, Ag|AgCl||3M KCl as a reference electrode and a Pt auxiliary electrode. All the electrochemical data were measured at room temperature in a 10 mL electrochemical cell at a scan rate of 50 mV/s. Sample homogenization was performed by a classic bar stirrer.

Prior to use, the working glassy electrode was polished with alumina powder and finally rinsed with Milli-Q water.

UV-Visible measurements were performed on a Varian DMS 80 (USA) spectrophotometer.

The particle size distribution measurement by dynamic light scattering method was performed with ZetaPlus (Brookhaven Instruments Corporation, USA). The same device was used for zeta-potential measurements.

Rheological evaluation of the prepared silver ink was carried out using an Ostwald viscometer and Traube stalagmometer.

The surface morphology and thickness of the printed silver lines were observed with a scanning electron microscope (Bruker, Germany).

The shape and particle size was determined by a Zeiss EM 10 A transmission electron microscope (Germany).

Ink homogenization was done on a Bandelin electronic (Germany) Sonorex high power ultrasound bath.

Hydrazine addition to the reaction mixture was carried out by a Gilson Minipuls Evolution peristaltic pump fitted with an MF4 pump head (France).

A digital Multimeter 34461A, 6 ½ Digit, Truevolt DMM, Keysight (USA) was used for resistance measurement.

2.3. Synthesis of silver nanoparticles

Ag nanoparticles were synthesized using N_2H_4 as the reducing agent and PAA as the protecting (capping) agent. The procedure can be described as follows:

1. step:

$$2AgNO_3(aq) + 2NaOH(aq) \rightarrow Ag_2O(s) + 2NaNO_3(aq) + H_2O(l) \qquad (1)$$
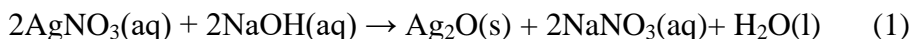
Silver nitrate (3.5 g) used as the Ag precursor was dissolved in 20 mL of water. To this solution, 25 mL of 1.15 M NaOH was added. The mixture was stirred for 10 minutes, and a brown–gray silver oxide precipitated. Next, the silver oxide precipitate was washed several times with water.

PAA was introduced as a silver capping agent to the precursor and reducing agent solutions. Both solutions were stirred vigorously for 10 minutes, before mixing them together. The molar ratio between PAA and Ag was 0.06.

2. step

$$2Ag_2O_{(s)} + N_2H_{4(aq)} \rightarrow 4Ag_{(s)} + N_{2(g)} + 2H_2O_{(l)} \qquad (2)$$
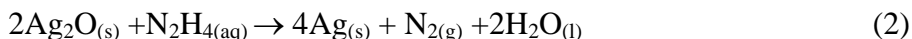
Fourteen milliliters of a hydrazine-PAA mixture was subsequently added to the Ag-PAA complex solution using the peristaltic pump in cycles of 20 seconds with 2 minutes of continuous stirring intervals between two additions. To ensure that the reaction had been completed, the concentration of the unreacted silver ions was determined by cyclic voltammetry. Hydrazine solution ($c = 0.383$ M) was added to the reaction mixture in small amounts by pipette, until a negative response to silver was obtained. The addition of hydrazine in equimolar portions increased the production yield of silver nanoparticles. After that, silver nanoparticles were precipitated by adding acetic acid ($V = 20$ mL, $c = 3$ M) to the reaction suspension. The use of weak organic acids for AgNP precipitation is a novelty, and the precipitation usually occurs by centrifugation or by the addition of large amounts of alcohol [50] or acetone [47]. After decantation, the precipitated nanoparticles were washed 3 times by water and finally 2 times by acetone. Then, the sediment was dried overnight at 60° C and the solid dust form of the silver nanoparticles was stored at room temperature in a glass vial.

2.4. Preparation of the stable silver nanoparticle ink suspension

Silver nanoparticle-based conductive ink with a solid loading of 25 wt% was prepared from the dried particles by redispersing them into an EG solution (20% wt) with the addition of a small amount of 2-AMP to adjust the solution's pH to 10.5. To ensure that the silver nanoparticles were being homogenously dispersed in the solvent, the whole suspension was kept in an ultrasonic bath for 2 hours.

Inkjet printing was carried out with an Epson Stylus D92 inkjet printer modified to work as a flatbed printer. Silver nanoink prepared as described was printed on paper or plastic substrates at room temperature. Line patterns of different length and width were printed for conductivity tests.

3. RESULTS AND DISCUSSION

3.1. Electroanalytical response of the glassy carbon electrode in silver solution

In this work, we evaluated the use of cyclic voltammetry with a glassy carbon electrode for monitoring the synthetic reaction between silver and hydrazine. Figure 1 shows the cyclic

voltammograms obtained with a glassy carbon electrode in a Britton-Robinson (BR) buffer solution at pH = 10.00 and with addition of silver nitrate at a scan rate of 50 mV/s.
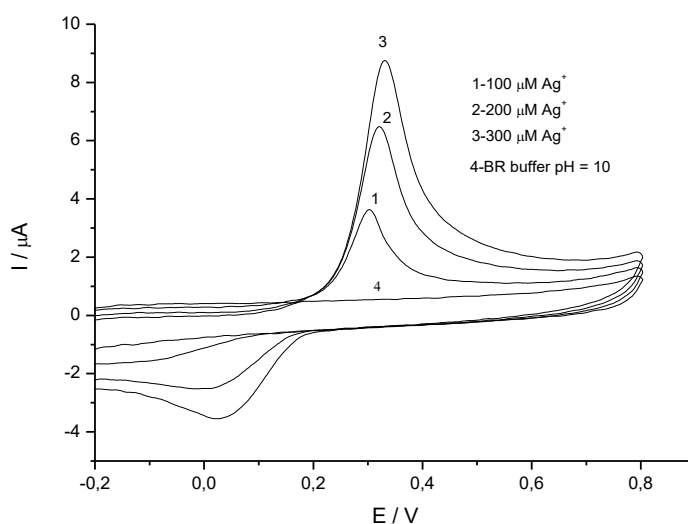

Figure 1. Cyclic voltammograms (CVs) recorded in the BR buffer solution (pH = 10.00), using a GC working electrode, Pt auxiliary electrode and Ag|AgCl||3M KCl reference electrode and a scan rate 50 mV/s. CVs denoted 1, 2 and 3 represent the response in silver solutions c(Ag) = 100, 200 and 300 μM, respectively.
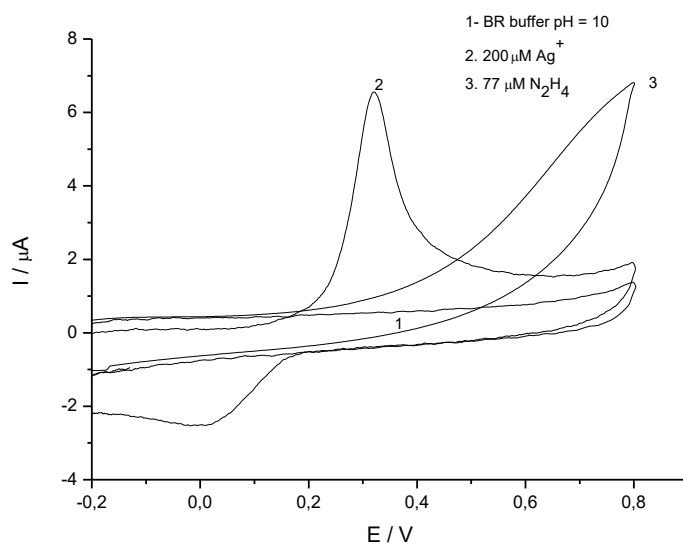

Figure 2. CVs recorded in the BR buffer solution (pH = 10.00). Measurement set up was the same as in Figure 1. Scan rate was 50 mV/s, c(Ag) = 200 μM, c(hydrazine) = 77 μM.

It is evident that in the whole range of tested potentials, no response was noted in the buffer solution (curve 4). In the solutions containing silver nitrate, anodic peaks are observed (peaks 1, 2, 3)

at potentials approximately 300 mV. The corresponding cathodic peaks are observed at potentials lower than 50 mV. The higher anodic current responses are obtained in solutions with higher silver concentrations. The relationship between the peak currents and silver ion concentration can be described as:

I_p / μA = (0.400 ± 0.187) + (0.022 ± 0.001) × c (Ag$^+$); R^2 = 0.997.

The cyclic voltammetric response obtained with the GC electrode in the BR buffer solution pH = 10.00, silver nitrate and hydrazine solutions are shown in Figure 2.

It can be seen that the oxidation processes of hydrazine on a glassy carbon electrode starts at a much higher potential and has no influence on silver detection. The presented results demonstrate the applicability of a glassy carbon electrode as a sensor for the detection of equivalence points in the redox reaction between silver and hydrazine.

Nanosilver preparation from silver oxide and hydrazine was performed by hydrazine addition in intervals lasting 20 seconds using a peristaltic pump. Near the equivalence point the pump was stopped, and the unreacted silver concentration was determined. The CVs recorded during synthesis are presented in Figure 3.
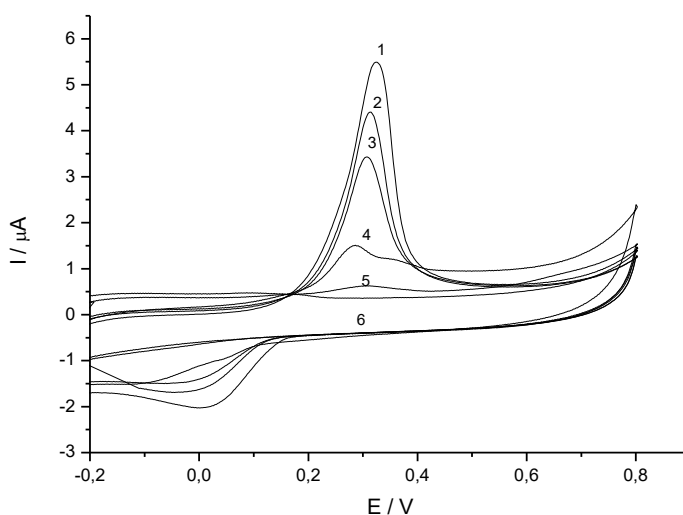

Figure 3. Cyclic voltammograms recorded in the primary buffer solution (pH = 10.00) after the addition of AgNPs (50 μL) to a 10 mL cell. The scan rate was 50 mV/s. Curves **1-5** represents c(Ag$^+$) existing in reaction during reduction, **6** – BR solution.

The first recorded CV (**1**) shows the existence of some unreacted silver, while the others (**2-5**) show a subsequent current decrease as a result of hydrazine addition to the reaction mixture. Continual addition of hydrazine causes a further decrease in the current response. Finally, when the equivalence point was reached, the current response became the same as obtained in the primary buffer solution.

Hydrazine is a highly toxic, reactive and explosive chemical [51], but it is still a widely used reduction agent in metal nanoparticle synthesis. While nanosilver syntheses using nontoxic reducing agents and stabilizing factors have been presented [52], our approach ensures a complete reaction and avoids the potential hazards of releasing either of the excess reactants into the ecosystem.

3.2. Electrochemical characterization of AgNPs stabilized by PAA

PAA stabilized AgNP samples obtained after the reaction with hydrazine were characterized by cyclic voltammetry and UV-Vis measurements. Figure 4 shows recorded CVs of the PAA stabilized Ag nanograins prepared in solutions of different pH.
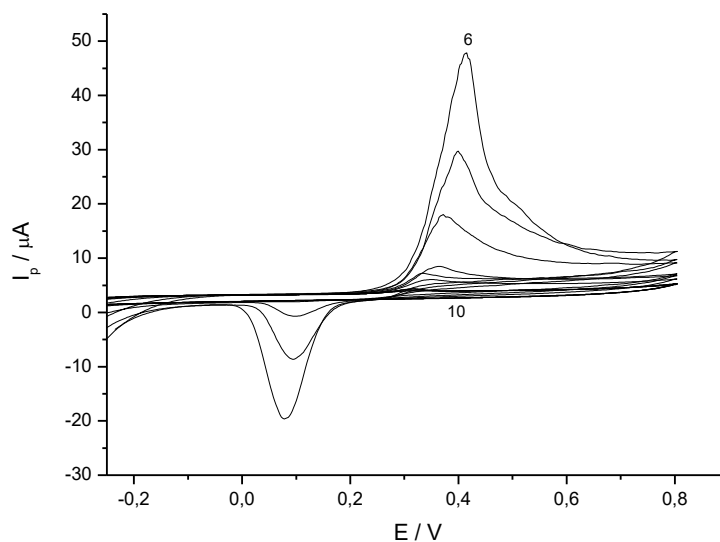

Figure 4. Hydrodynamic CVs of PAA stabilized AgNPs obtained after 150 µL conductive ink addition into a 10 mL BR buffer solution at various pH values. The pH range is 10.00 (line marked 10) to 6.00 (line marked 6) with 0.5 pH unit increments.

PAA adsorbed on AgNP surface behaves as a weak acid and was totally deprotonated in the alkaline medium. Fully deprotonated PAA adsorbed on AgNP surface generates a negative surface charge, which influences the coulombic repulsion force between nanograins. The efficiency of the electrostatic stabilization depends on the acid dissociation rate. Therefore, to study the effect of pH on the stability of the AgNPs, hydrodynamic CVs were recorded in the pH range between pH = 10.00 and pH = 4.50. CVs recorded from pH = 10.00 to pH = 6.00 are shown in Figure 4. Recording CVs started at a negative potential. At negative potentials and high pH values, the repulsion force between the polarized electrode and negatively charged AgNPs results in minor current responses (curve **1**). However, at lower pH values the PAA dissociation rate decreases, which reduces the repulsion force between the electrode and nanograins. Higher current responses are obtained from the CVs. The maximum anodic current is observed at pH = 6 (curve **6**).
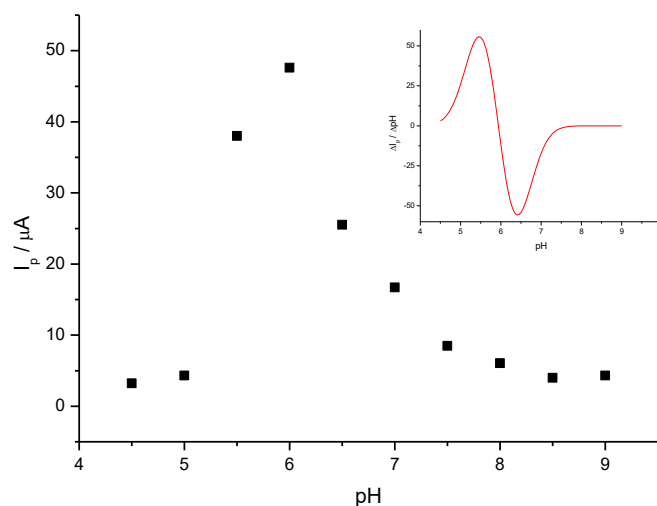
Figure 5. The dependence of the peak current on pH for data shown in Figure 4. Inset: first derivative of the data.

At pH = 5.00, all of the PAA is fully protonated, and the silver nanograins become partially precipitated. This behavior results in a significant decrease in the current response below pH = 6.00. Figure 5 shows the results of the highest peak current *vs* pH. The current intensity depends on the nanosilver concentration, the quantity of adsorbed PAA stabilizer, and pH. The presented curve can be used for surface bound PAA constant dissociation rate determination. The first derivative of the data (Figure 5 inlay) indicates the function trough at pH = 6.40, which generates the pK_a value of the polyelectrolyte. This calculated value of the adsorbed PAA dissociation constant shows a difference from data obtained for acrylic acid monomers in aqueous solution (pK_a = 4.50) [53], but it is in good agreement for the aqueous polymer solution (pK_a = 6.50) [54]. This result also confirmed that precipitation by acetic acid was efficient and did not influence the properties of the adsorbed PAA. It is necessary to use protective agents to stabilize the metal nanoparticles during their preparation procedure. CV can confirm the existence of PAA on the nanometal surface, but the protective efficiency in the ink formulation must be additionally confirmed by zeta potential measurements.

3.3. Optical characterization of AgNPs stabilized by PAA

Within the silver nanoparticles, the conduction and valence band overlap, and electrons move easily. After electrons interact with light, the free electrons become distributed into a surface plasmon resonance (SPR) absorption band. This absorption strongly depends on the size, shape and degree of particle agglomeration. Experimentally and theoretically, it has been discovered that when size decreases, the SPR peak shifts toward shorter wavelengths. It was also found that as the nanoparticle size increases, the absorption spectra become less intense and wide-ranging [55].
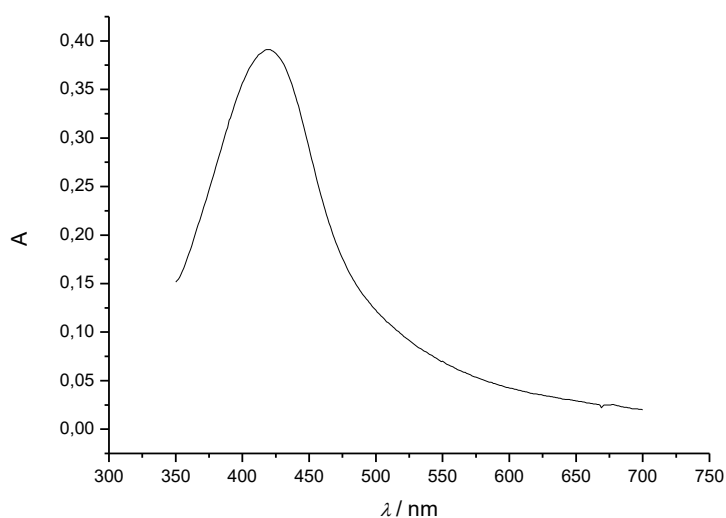
Figure 6. UV-Vis absorption spectrum of the prepared PAA-AgNP sample, recorded at the end of synthesis. Sample dilution $\varphi = 1{:}10000$.

Figure 6 shows the UV-Vis absorption spectrum of the PAA stabilized AgNP sample, recorded before precipitation. The absorption peak of the pale yellow silver colloids was in the visible range with a maximum at 417 nm. This finding indicates the presence of spherical AgNPs in the specimen, which was also confirmed by TEM imaging. The spectrum has a symmetrical shape, which is characteristic for narrow particle-size distributions. The stability of the prepared ink with silver content ($w = 25\%$) was tested over the course of 7 months. Figure 7 shows the UV-Vis spectra recorded during the seven month testing period.
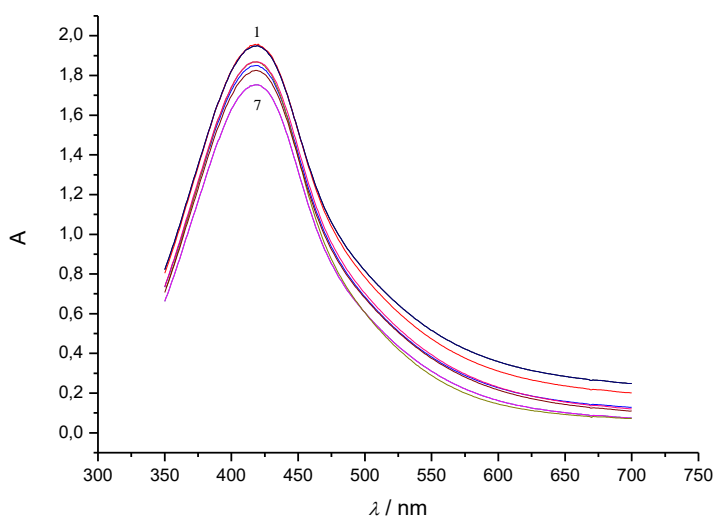

Figure 7. UV-Vis absorption spectrum of PAA-stabilized AgNPs in a conductive ink formulation during a testing period of seven months. **1-7** designate the number of months.

It is evident from Figure 7 that the absorption peak remains at the same wavelength during the testing period, and it is in accordance with the SPR absorption maximum presented in the previous

Figure. The UV-Vis spectra show a symmetrical shape with a narrow absorption peak. The slight reduction in the peak absorption intensity is caused by the adsorption of the nanoscale silver on the glass wall of the vial that the ink was kept in.
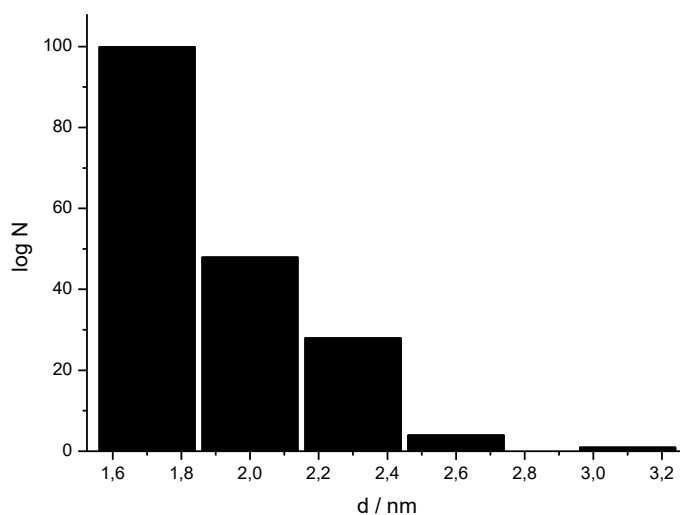
3.4. TEM, DLS and zeta-potential analysis

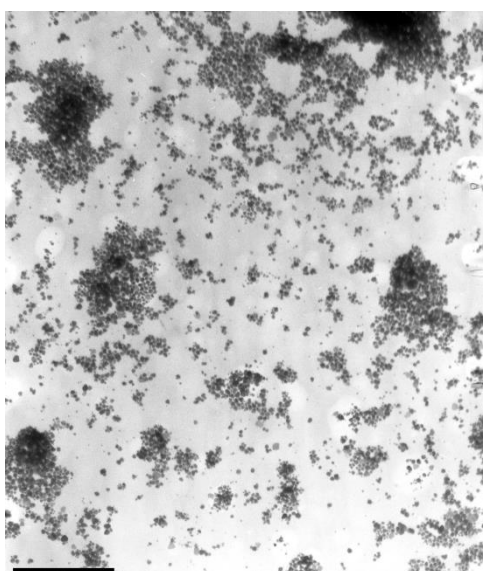**Figure 8.** Particle size distribution of PAA-stabilized AgNPs in ink formulation. Sample dilution $\varphi = $ 1:40000.

Figure 9. TEM image of the prepared nanosilver ink formulation measured with magnification 25000×. Inserted bar represents a 0.5 µm scale.

The particle shape and size distribution were investigated by DLS (Figure 8) and TEM (Figure 9). It is evident from the particle size histogram that in the tested sample a large number of small

AgNPs are present at diameters between 1.6 and 3.2 nm. The AgNPs synthesized according to this procedure are much smaller than the AgNPs intended for inkjet printing found in the literature [47,50,56]. Despite their small size, the tendency of the particles in the conductive ink to form agglomerates can cause clogging of printer nozzles [57]. Therefore, the stability of the PAA-AgNP conductive ink has been determined by a measurement of the electrokinetic potential. The zeta potential analysis can give the tendency of the particles to agglomerate or to precipitate. The measured value of the zeta potential was -52.83 ± 1.29 mV, suggesting suitable ink stability. Figure 9 represents a TEM image of the prepared material, which indicates that the AgNPs have some agglomerates of spherical shape. However, such small agglomerate sizes do not affect quality of printed patterns.

3.5. Resistivity of printed features

Using the conductive ink, a silver electrode (Figure 10) was printed on a flexible substrate and then sintered at 105 °C for 20 minutes. The next step involved measuring the resistance of the electrode line at room temperature using a four point technique. The line thickness (h) needed for the resistivity calculations was measured by means of an SEM (scanning electron microscope) cross-section image (Figure 11).
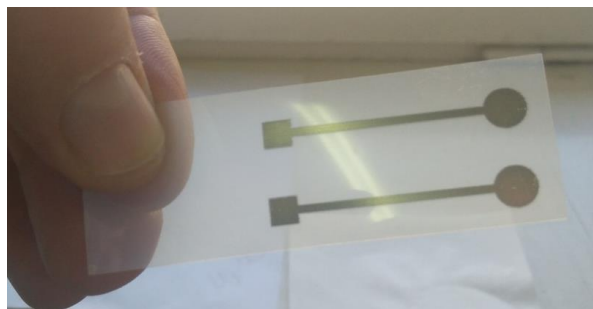

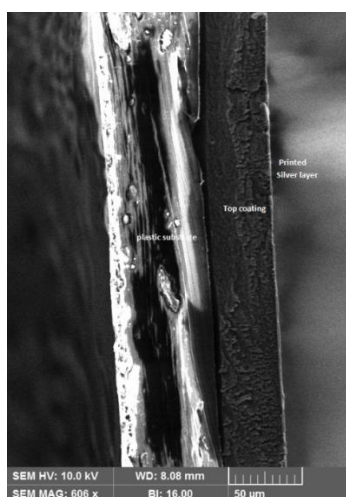**Figure 10.** Printed nanosilver electrodes

Figure 11. SEM cross-section image of the printed silver track on a flexible plastic substrate after sintering.

The resistivity was calculated using the equation: $\rho = (R{\times}b{\times}h) / l$ [58], where R is the resistance, b is the width of the printed Ag line, h is the thickness, and l is the line length. Thickness (h) was determined as the average value of thickness measurements using the SEM cross-section image performed at ten different places. The calculated value for resistivity of the prepared ink was 8.0×10^{-8} Ωm, approximately 4.76 time greater than that of bulk silver (1.68×10^{-8} Ωm) [59].

4. CONCLUSION

The method we described was based on the chemical reduction of silver nitrate using hydrazine monohydrate as a reducing agent. The size and stability of the obtained silver nanoparticles was coordinated by the existence of poly(acrylic acid). The obtained silver nanoparticles were an order of magnitude smaller than the AgNPs for printing applications found in the literature. The silver nitrate concentration was controlled during nanosilver preparation by cyclic voltammetry, not only to obtain a large amount of nanosilver as a product of the chemical reaction but also as a means of environmental protection from silver ion bioinfluence. Hydrazine hydrate, which is used in the chemical reduction process for the preparation of nanosilver, can also cause damage to aquatic systems. Cyclic voltammetry can be successfully applied for concentration control of both used reactants. The majority of the wet nanosilver syntheses described to date provide a stable dispersion of metal nanoparticles prepared from highly diluted solutions, which is not suitable for large scale production. The synthesis we described is based on using concentrated solutions.

According to the literature, nanosilver precipitation has been mainly done by centrifugation or by the addition of large amounts of alcohol (methanol, ethanol, propanol) or acetone. The preparation of silver nanopowder precipitated by acetic acid was successfully applied in this work. The dispersion of AgNPs containing a metal content of $w(\text{Ag}) = 25\%$ was stable during the seven months of testing. The applicability of the prepared ink was confirmed by printing different shapes and functional electrodes using an inkjet printer.

AUTHOR CONTRIBUTIONS
S.M. developed the whole idea and prepared the manuscript. I.I. carried out all synthesis experiments and UV-Vis measurements, A.R. performed the SEM and DTG measurements, while P.K. carried out inkjet printing on flexible substrates and revised the manuscript. None of the authors have any competing interest in this manuscript.

References

1. V. Pareek, R. Gupta and J. Panwar, *Mater. Sci. Eng.*, C, 90 (2018) 739.

2. J. S. Möhler, W. Sim, M. A. T. Blaskovich, M. A. Cooper and Z. M. Ziora, *Biotech. Adv.*, 36 (2018) 1391.
3. N. Elahi, M. Kamali and M. H. Baghersad, *Talanta,* 184 (2018) 537.
4. M. Gatalo, P. Jovanovič, F. Ruiz-Zapeda, A. Pavlišić, A. Robba, M. Bale, G. Dražić, M. Gaberšček and N. Hodnik, *J. Electrochem. Sci. Eng.*, 8 (2018) 87.
5. I. Mintsouli, J. Georgieva, A. Papaderakis, S. Armyanov, E. Valova, V. Khomenko, S. Balomenou, D. Tsiplakides and S. Sotiropoulos, *J. Electrochem. Sci. Eng.*, 6 (2016) 17.
6. S. H. Kim, *Curr. App. Phys.*, 18 (2018) 810.
7. A. Cernikova, J. Donhal and J. Jampilek, *ADMET DMPK*, 3 (2015) 345.
8. V. Subramanian, J. M. J. Frechet, P. C. Chang, D. C. Huang, J. B. Lee, S. E. Molesa, A. R. Murphy, D. R. Redinger and S. K. Volkman, *Proc. IEEE*, 93 (2005) 1330.
9. D. Newman, A. P. F. Turner and G. Marrazza, *Anal. Chim. Acta*, 62 (1992) 13.
10. M. O'Toole, R. Shepherd, G. G. Wallace and D. Diamond, *Anal. Chim. Acta,* 652 (2009) 308.
11. T. R. Hebner, C. C. Wu, D. Marcy, M. H. Lu and J. C. Sturm, *Appl. Phys. Lett.*, 72 (1998) 519.
12. D. Huang, F. Liao, S. Molesa, D. Redinger and V. Subramanian, *J. Electrochem. Soc.*, 150 (2003) G412.
13. M. Hilder, B. Winther-Jensen, N. B. Clark, *J. Power Sources*, 194 (2009) 1135.
14. S. B. Fuller, E. J. Wilhelm and J. M. Jacobson, *J. Microelectromech. Syst.*, 11 (2002) 54.
15. D. L. MacFarlane, V. Narayan, J. A. Tatum, W. R. Cox, T. Chen and D. J. Hayes,, *IEEE Photon. Technol. Lett.*, 6 (1994) 1112.
16. H. Andersson, A. Manuilsky, J. Siden, J. Gao, M. Hummelgård, G. V. Kunninmel and H. E. Nilsson, *Mater. Res. Express*, 1 (2014) 035021.
17. N. L. Pacioni, C. D. Borsarelli, V. rey and A. V. Veglia, Silver Nanoparticle Application in the Fabrication and Design of Medical and Biosensing Devices, Springer International Publishing, (2015) Switzerland.
18. F. Mafune, J. Kohno, Y. Takeda, T. Kondow, H. Sawabe, *J. Phys. Chem.* B, 105 (2001) 5114.
19. S. A. Kumar, A. Majid Kazamian, S. W. Gosavi, K. K. Sulabha, P. Renu, A. Ahmad and M. I. Khan, *J. Biotechnol. Lett.*, 29 (2007) 439.
20. V. K. Sharma, R. A. Yngard and Y. Lin, *Adv. Colloid Interface Sci.*, 145 (2009) 83.
21. S. S. Shankar, A. Absar and S. Murali, *Biotechnol. Prog.,* 19 (2003) 1627.
22. B. Wiley, Y. Sun, B. Mayers and Y. Xi, *Chem. Eur. J.,* 11 (2005) 454.
23. K. A. El-Nour, A. F. Eftaiha, A. Al-Warthan and R. A. A. Ammar, *Arabian J. Chem.*, 3 (2010) 135.
24. G. Suriati, M. Mariatti and A. Azizan, *Int. J. Automot. Mech. Eng.,* 10 (2014) 1920.
25. K. S. Chou and C. Y. Ren, *Mater. Chem. Phys.*, 64 (2000) 241.
26. A. I. Wasif, S. M. Landage and P. U. Dhuppe, *Int. J. Adv. Res. Eng. Appl. Sci.*, 3 (2014) 44.
27. C. C. Li, S. J. Chang, F. J. Su, S. W. Lin and Y. C. Chou, *Colloids Surf.* A, 419 (2013) 209.
28. G. Zhou and W. Wang, *Orient. J. Chem.*, 28 (2012) 651.
29. J. Turkevich, P. C. Stevenson and J. Hillier, *Disc. Faraday Soc.,* 11 (1951) 55.
30. D. Steinigeweg and S. Schlücker, *Chem. Commun.*, 48 (2012) 8682.
31. D. L. Van Hyning and C. F. Zukoski, *Langmuir*, 14 (1998) 7034.
32. D. Ghosh and S. Dasgupta, *Metall. Mater. Trans.* B, 39 (2008) 35.
33. M. V. Cañamares, J. V. Garcia-Ramos, J. D. Gómez-Varga, C. Domingo and S. Sanchez-Cortes, *Langmuir*, 21 (2005) 8546.
34. Y. Sun, Y. Yin, B. T. Mayers, T. Herricks and Y. Xia, *Chem. Mater.*, 14 (2002) 4736.
35. D. Kim, S. Jeong and J. Moon, *Nanotechnology*, 17 (2006) 4019.
36. J. Y. Lin, J. L. Hsueh and J. J. Huang, *J. Solid State Chem.*, 214 (2014) 2.
37. J. Pulit and M. Banach, *Dig. J. Nanomater. Biostruct.*, 8 (2013) 787.
38. M. Olivera, D. Ugarte, D. Zanchet and A. Zarabin, *J. Colloid Interface Sci.*, 292 (2005) 429.
39. A. Majid and F. Bensebaa, *Rev. Adv. Mater. Sci.*, 4 (2003) 25.
40. K. Yoshida and P. L. Dubin, *Colloids Surf.* A, 147 (1999) 161.

41. S. W. Cranford, C. Ortiz and M. J. Buehler, *Soft Matter*, 6 (2010) 4175.
42. A. Fahmy, W. H. Eisa, M. Yosef and A. Hassan, *J. Spectrosc*., 5 (2016) 1.
43. Y. C. Lu and K. S. Chou, *J. Chin. Inst. Chem. Eng*., 39 (2008) 673.
44. J. D. S. Newman and G. J. Blanchard, *Langmuir*, 22 (2006) 5882.
45. S. M. I. Morsy, *Int. J. Curr. Microbiol. App. Sci.,* 3 (2014) 237.
46. K. Szczepanowicz, J. Stefańska, R.P. Socha and P. Warszyński, *Physicochem. Probl. Miner. Process.*, 45 (2010) 85.
47. B. Y. Ahn and J. A. Lewis, *Mater. Chem. Phys*., 148 (2014) 686.
48. B. H. Ryu, Y. Choi, H. S. Park, J. H. Byun, K. Kong, J. O. Lee and H. Chang, *Colloids Surf*. A, 270-271 (2005) 345.
49. A. Kamyshny, J. Steinke and S. Magdassi, *TOAPJ*, 4 (2011) 19.
50. Q. Huang, W. Shen, Q. Xu, R. Tan and W. Song, *Mater. Chem. Phys*., 147 (2014) 550.
51. M. George, K. S. Nagaraja and N. Balasubramanian, *Indian J. Chem., Sect. A: Inorg., Bio-inorg., Phys., Theor. Anal. Chem.*, 46A (2007) 1621.
52. M. Banach and J. Pulit, *Chemik,* 68 (2014) 111.
53. M. Wiśniewska, T. Urban. E. Grządka, V. I. Zarko and V. M. Gun'ko, *Colloid Polym. Sci.,* 292 (2014) 699.
54. S. W. Cranford, C. Ortiz and M. J. Buehler, *Soft Matter*, 6 (2010) 4175.
55. J. A. Creighton and D. G. Eadon, *J. Chem. Soc. Faraday Trans*., 87 (1991) 3881.
56. W. Shen, X. Zhang, Qijin Huang, Q. Xu and W. Song, *Nanoscale*, 6 (2014) 1622.
57. A. Lee, K. Sudau, K. H. Ahn, S. J. Lee and N. Willenbacher, *Ind. Eng. Chem. Res.*, 51 (2012), 13195
58. F. Wang, P. Mao and H. He, *Sci. Rep*., 6 (2016) 1.
59. J. R. Greer and R. A. Street, *Acta Mater*., 55 (2007) 6345.